Monitoring protein aggregation and toxicity in Alzheimer's disease mouse models using in vivo imaging

Published in final edited form as:
Methods. 2011 March ; 53(3): 201–207. doi:10.1016/j.ymeth.2010.12.009.

Monitoring protein aggregation and toxicity in Alzheimer's disease mouse models using in vivo imaging

Tara L Spires-Jones[a], **Alix de Calignon**[a,1], **Melanie Meyer-Luehmann**[a,2], **Brian J Bacskai**[a], and **Bradley T Hyman**[a]

[a] Massachusetts General Hospital/ Harvard Medical School, 114 16th Street, Charlestown, MA USA 02148

Abstract

Aggregation of amyloid beta peptide into senile plaques and hyperphosphorylated tau protein into neurofibrillary tangles in the brain are the pathological hallmarks of Alzheimer's disease. Despite over a century of research into these lesions, the exact relationship between pathology and neurotoxicity has yet to be fully elucidated. In order to study the formation of plaques and tangles and their effects on the brain, we have applied multiphoton in vivo imaging of transgenic mouse models of Alzheimer's disease. This technique allows longitudinal imaging of pathological aggregation of proteins and the subsequent changes in surrounding neuropil neurodegeneration and recovery after therapeutic interventions.

Keywords

Alzheimer; tau; plaque; multiphoton; in vivo imaging

1. Introduction

Alzheimer's disease (AD), first described in 1907, is a devastating neurodegenerative disorder characterized by dementia and pathologically defined by the presence of 2 types of abnormal protein aggregates: intracellular neurofibrillary tangles (NFT) and extracellular senile plaques (1). Plaques are composed largely of aggregated amyloid beta peptide (Aβ) derived from proteolytic cleavage of amyloid precursor protein (APP), while NFT are formed of hyperphosphorylated and misfolded tau protein (2). Pathological protein aggregation is a common feature across the spectrum of neurodegenerative diseases, thus it is important to elucidate the relationship between protein aggregation and degeneration of the brain in order to develop therapeutic strategies.

In AD, the presence of plaques is an early occurrence in the disease process and mutations in amyloid precursor protein and presenilins 1 and 2, proteins involved in cleaving APP to generate Aβ, can cause rare familial forms of AD strongly implicating amyloid as the

Corresponding Author: Tara L Spires-Jones, 114 16th Street, Charlestown, MA 02129, 1(617)724-8330, Fax 1(617)724-1480, tspires@partners.org.
[1]Present address: University of Oxford, Department of Physiology, Anatomy, and Genetics, Oxford, UK
[2]Present address: 1) German Center for Neurodegenerative Diseases (DZNE), 80336 Munich, Germany; 2) Adolf-Butenandt-Institute, Biochemistry, Ludwig Maximilians-University, 80336 Munich, Germany

initiating factor in the disease (3). NFT accumulate and spread through the brain later in the disease process, however their presence correlates better with cognitive decline, synapse loss, and neuronal loss than amyloid burden, arguing the importance of NFT in the degenerative process (4). These post-mortem data implicating amyloid in disease initiation and NFT in neuronal death are correlative and not definitive since by their nature these experiments cannot determine the precise timing and order of events. Using transgenic mouse models that accumulate plaque or tangle pathology, we have developed a method combining *in vivo* multiphoton imaging of pathology with viral infections to fill neurons with fluorophores, proteins postulated to be involved in neurodegeneration, or functional indicators to study the timing of plaque and tangle formation and the degeneration associated with them (see outline of the method in figure 1).

2. Materials and Methods

2.1 Animal models

In order to study aggregation of Alzheimer-related proteins, we take advantage of transgenic mouse models expressing human amyloid precursor protein, presenilin, or tau with mutations associated with familial forms of AD or frontotemporal dementia. We have used several plaque-bearing mouse models including Tg2576 mice which express the 695 amino acid isoform of APP containing the 'Swedish' double mutation Lys670-Asn, Met671-Leu (5), PDAPP mice expressing an APP minigene with the V717F mutation (6), and APP/PS1 mice expressing a mutant human presenilin 1 (DeltaE9) and a chimeric mouse/human APP with the Swedish double mutation (7). These mice all develop senile plaques but at different ages and on different strain backgrounds, so investigating aggregation across several models allows confirmation of the relevance of findings to the disease pathogenesis. We study NFT formation and toxicity in the rTg4510 mouse model expressing human tau with the P301L mutation associated with frontotemporal dementia (8). This model has the advantage of being regulatable – the transgene can be suppressed with doxycycline administration in the food – allowing investigation of the reversibility of effects of NFT on the brain.

Transgenic mouse models not directly related to Alzheimer's pathology are also very useful for imaging the effects of AD pathology on the brain when crossed with AD model mice. For example, animals transgenic for fluorescent proteins can be used to study the effects of pathology on neuronal structure (9), mice expressing immediate early genes could be used to asses the response of neurons to stimulation (10), mice with fluorescent mitochondria could be used to study the effects of pathology on mitochondrial localization (11), mice with fluorescent microglia have been used to observe glial changes around plaques (9,12), etc.

All animal work described here conforms to NIH and institutional IACUC regulations.

2.2 Instrumentation

2.2.1 Surgical equipment—For surgery and imaging, the mouse must be anesthetized and the head stabilized in a stereotaxic device. Since these are long-term experiments, we are careful not to place the ear bars into the ears of the animal to avoid rupturing the tympanic membranes which is painful for the animal. Instead ear bars are placed in the notch on the skull immediately anterior to the ears. For injection of virus into the brain, a standard stereotaxic frame with a syringe holder and pump are ideal (stereotaxic apparatus - David Kopf instruments. Tujunga, CA; injector system - Stoelting Co, Wood Dale, IL). Similarly, for craniotomy and cranial window implantation, standard stereotaxic devices can be used. For imaging on the microscope, specialized stereotaxic frames mounted on a base that fits into the microscope stage can be used, or a small steel bar with a screw hole can be

implanted adjacent to the cranial window and a small screw used to secure the animal onto a holder mounted on the microscope stage (13).

For cranial window implantation, we use a dissecting scope (for example Zeiss, Stemi SV6) to visualize the surgical area and use illuminators with light guides (Fiber Light, Dolan-Jenner Industries, Boxborough, MA). Standard microsurgical tools are used (from Fine Science Tools and Harlan Tekland).

2.2.2 Multiphoton microscope system—Imaging with two-photon laser excitation allows penetration of the laser to subcortical areas up to several hundreds of microns deep (to layer V) without phototoxicity that would be induced by visible light lasers. For in vivo multiphoton imaging, we have used 2 systems, (1) a BioRad 1024 system mounted on an upright Olympus BX50WI microscope with a custom built three channel photomultiplier array and (2) an Olympus Fluoview 1000MPE mounted on an Olympus BX61WI upright microscope with four photomultiplier detectors. Both systems use a mode-locked tunable femtosecond pulsed titanium/sapphire laser (Mai Tai, Spectraphysics) for excitation. A 20× high numerical aperture (0.95) dipping objective is used due to its long working distance and large light gathering capacity.

2.3 Surgical Procedures

The specialized surgical techniques for in vivo imaging are difficult to replicate based on written procedures. Several groups around the world specialize in this type of imaging and regularly train scientists in the surgical techniques. Watt Webb from Cornell and Winfried Denk at the Max Planck Institute first implemented multiphoton microscopy for imaging live cells. Other investigators routinely using cranial window implantation and multiphoton imaging of the brain include Karel Svoboda at Howard Hughes Medical Institute (13), and Mark Hubener and Tobias Bonhoeffer at the Max Planck Institute (14). There are also video protocols that are very useful in learning the technique that have been published in the Journal of Visualized Experiments (15–17).

Before surgical procedures, sterilize the work area and stereotax with 70% ethanol. Surgical instruments should be sterilized in a bead sterilizer. Prepare sterile PBS on ice and soak gel foam cut into small squares (2–3mm) in sterile PBS for keeping the skull moist.

2.3.1 Anesthesia—Either injection or inhalant anesthetics may be used for surgery and repeated imaging of animals, however, several factors should be considered before choosing an anesthetic regimen. It is important to maintain body temperature near 37C particularly in tau expressing animals since hypothermia has been shown to enhance tau phosphorylation (18). Isoflurane, a commonly used inhalant anesthetic is more dangerous to workers than injectibles (particularly pregnant women) since they are exposed to some amounts of the anesthetic which is known to have detrimental effects on the developing brain (19). With that caveat, we have found that isoflurane is a good choice of anesthetic since body temperature can be maintained, maintenance of anesthesia for imaging can be done with low levels of anesthetic (below 1% in oxygen), animals recover very quickly from anesthesia, and we have very low levels of morbidity associated with isoflurane anesthesia compared to avertin or ketamine/xylazine. We use isoflurane in oxygen administered via a mask that fits onto the stereotaxic device from a vaporizer set to 3% for induction (in a chamber) then reduced to 0.5–2% for maintenance of anesthesia (through the mask). Excess isoflurane is scavenged using a hood system in surgical areas and with a vacuum line on the microscopes to minimize human exposure.

Ketamine/xylazine (100mg/kg ketamine, 1mg/kg xylazine) administered intraperitoneally can also be used. If anesthetic depth is too low, top up doses of ketamine (without xylazine)

can be administered. In both cases, depth of anesthesia is monitored every 5 minutes by toe pinch response or observing respiration rate. While anesthetized, body temperature is maintained with homeothermic blankets and monitored with a temperature probe (Harvard apparatus, Holliston, MA). Animals recover on the heating blanket. If they have been anesthetized for over 3 hours, a dose of warm, sterile PBS is administered i.p. (300 μL) to warm and hydrate the mouse during recovery.

2.3.2 Intracortical injections—Injection of adeno-associated virus or lentivirus can be used to introduce genes of interest including fluorescent markers for anatomical studies (20), functional markers such as calcium indicators (21), potential therapeutic proteins (22), or Alzheimer-related proteins such as tau to study aggregation and toxicity (23,24). For this procedure, biosafety precautions appropriate for the biohazard potential of each virus should be used, (lab coat, gloves, mask, etc) as outlined in the manual: Biosafety in Microbiological and Biomedical Laboratories 5th Edition: Center for Disease Control and National Institutes of Health (25).

Animals are anesthetized and placed in a stereotaxic apparatus (David Kopf instruments. Tujunga, CA) with an injector system (Stoelting Co, Wood Dale, IL). Body temperature is maintained with heating pads as described in section 2.3.1. The scalp is shaved then cleaned with alternating coats of betadyne and isopropyl alcohol. Lidocaine (xylocaine 2%, Willard, OH) is injected subcutaneously as a local anesthetic. A small incision (approximately 2–3mm) is made along the midline of the scalp just posterior to the level of the ears and microdissecting hooks used to hold the skin out to the sides. The periosteum is removed with cotton tipped applicators and a surgical marker used to mark the sites on the skull for injection. Any dorsally located cortical region can be targeted, but we typically inject in primary somatosensory cortex (hind limb) which is accessible from a cranial window of 6mm diameter on the center of the skull. Coordinates of this area are 1mm lateral from the midline and 0.5mm posterior to the Bregma suture. The skull should remain moist throughout the procedure using PBS-soaked Transgel™.

A micro drill with 0.45 mm burr tip (VWR) is used to make a burr hole through the skull at the injection sites (multiple sites can be injected in one sitting, for example bi- lateral injections into S1). For each virus used, pilot testing will be needed to determine the amount of virus to inject for a good infection rate. In our hands, AAV with a titer of approximately 10^{12} viral genomes/mL works with 2 μL of virus injected per site. The virus is loaded into a 10 μL Hamilton syringe (Hamilton Co, Reno, NV) and the needle placed in the first burr hole until the tip of the needle touches the dura. From this level, the needle is lowered to 0.5mm deeper than the intended target depth. For example, to infect layer V neurons, the needle is lowered 1.5mm into the cortex. The needle is allowed to rest for 1 minute at this depth then raised 0.4mm, rest 1 minute and begin injecting the virus at 0.2 μL/min. After all of the virus is injected, rest 3 minutes, raise the needle half way to the surface (0.55mm), rest 3 minutes, then withdraw entirely from the cortex. This slow withdrawal of the needle prevents the virus-containing liquid from following the needle up through the cortex.

Repeat this procedure at all injection sites then suture or staple the skin closed and apply antibiotic ointment to the wound. Animals recover from anesthesia on a heating pad then are returned to the home cage. Virus should be allowed to express for several weeks before cranial window implantation and imaging.

2.3.3 Cranial Window Implantation—To install a cranial window, animals are anesthetized and placed into a stereotaxic device to stabilize the head. The scalp is shaved, cleaned and local anesthetic administered as described for injections in section 2.3.2. The scalp is removed from the dorsal surface of the head with small scissors to expose the entire

dorsal surface of the skull. Periosteum is removed with several cotton-tipped applicators. After this stage, the skull should be kept moist with PBS-soaked gel foam except over areas that are being drilled. With the drill, a shallow circle approximately 6mm in diameter is lightly scored starting just anterior to Bregma and ending anterior to lambda. The circle is then drilled through in small segments until the skull is transparent, taking care to keep the area cool with frequent applications of chilled PBS. Any bleeding in the skull is stopped by applying gel foam and removing excess liquid with absorbent triangles (Kettenbach, Eschenburg, Germany). When the entire circle has been drilled, the skull flap is gently removed with angled forceps exposing the surface of the brain, and PBS-soaked gel foam is immediately applied to absorb any bleeding resulting from the removal of the skull. If there is bleeding, clean gel foam is applied frequently and excess liquid absorbed with absorbent triangles until all liquid absorbed is clear indicating the bleeding has stopped.

If a topical agent is being applied (for example thioflavin S to label neurofibrillary tangles or a caspase indicator (24,26), dura are resected with fine forceps to allow the dyes to access the brain. Topical agents are left to incubate on the brain under plastic wrap for 20–30 minutes with a foil cover to protect the area from light. The brain is then rinsed with PBS before closing the window site.

The craniotomy is permanently sealed by placing a 7 or 8 mm glass coverslip (Warner Instruments, Hamden, CT) over the site, filling under the coverslip with PBS, then sealing the coverslip onto the skull with a mixture of dental acrylic (Jet Denture, Lang Dental Manufacturing, Wheeling, IL) and krazy glue ™ applied with a toothpick. A temporary seal can also be used (KwikKast, WPI Sarasota, FL) if multiple agents are applied topically in the same session, for example imaging, applying antibodies to remove soluble amyloid beta, then re-imaging (27). To use a head stabilizer that is directly attached to the microscope stage, a small metal bar with a screw hole is cemented adjacent to the cranial window (13).

If imaging is necessary immediately, the animal can be transferred directly to the microscope after sealing the craniotomy without waking from anesthesia. When topical agents are not used, it is preferable to allow the animal to recover and heal after craniotomy for several weeks before imaging to avoid observing any glial activation due to the surgery (13).

2.4 Imaging

2.4.1 Dyes to label pathology and structures affected by pathology—A key to multiphoton imaging in vivo is labeling structures of interest with fluorescent reporters to make them detectable with the technique. As mentioned in section 2.3.2, fluorophores can be introduced into brain cells using viral infections, and transgenic animal models with fluorescent reporters can be used for imaging. Fluorophores can also be introduced via topical application to the surface of the brain or systemic injections as detailed below.

To label amyloid plaques in APP or APP/PS1 transgenic mice, methoxy XO4 (courtesy William Klunk, Pittsburgh) is injected i.p. approximately 18 hours prior to imaging. Methoxy XO4 in injected at 3.3 mg/kg, from a 10 mg/mL stock in DMSO dissolved in cremophor EL (Fluka) and PBS (10 μL methoxy XO4 stock in 20 μL cremophor topped up with PBS to make 300 μL final volume). PIB can also be used to label plaques (28).

To label tangles, thioflavin S is applied topically at 0.025% in sterile PBS during cranial window implantation surgery (26) or X34 can be injected 2 hours before imaging in a lateral tail vein (0.03% X-34 in PBS, gift from Dr. W.E. Klunk) (24). We have also observed NFT in vivo after i.v. injection of FSB following the method of Velasco et al. (29).

Markers of structures and physiological processes that can be affected by pathology can also be used. The detailed methods for all of these will not be included here but in general the dyes can be introduced by virus or administered topically or via i.p. or i.v. injection as described in sections 2.3.2 and 2.3.3 and references can be found in table 1.

Some treatments to clear pathology, such as anti Aβ antibodies, can be fluorescently tagged to allow monitoring of the treatment along with its effects on pathology. These labeled antibodies are applied topically to the brain at approximately 1 mg/mL during cranial window implantation (27,30). Of course, unlabelled treatments (drugs, etc) can also be administered, and the long term effects of the treatments on pathology can be observed.

It is worth noting that reagents which can cross the blood-brain-barrier and be administered systemically (i.p. or i.v.) are much better than those that must be applied topically onto the brain at the time of window implantation as they allow repeat imaging over weeks and months. These also uniformly label the entire cortex whereas topical agents penetrate slowly and only reach depths of approximately 200 μm. Topical agents can only be applied once, when the window is installed, since removing the window causes too much damage to the brain and almost always results in hemorrhage rendering the window useless for imaging. On the other hand, topical application of dyes and targeted infection with AAV have the advantage of not affecting the rest of the body thus isolating any effects seen as truly related to the cortex.

2.4.2 Angiogram—A fluorescent angiogram is useful for finding the same imaging sites in multiple imaging sessions. Texas Red dextran (50,000 mw, 12.5 mg/mL in PBS) or any other fluorescently labeled dextran is injected into a lateral tail vein immediately before imaging. The dye is cleared from the vessels several hours after injection.

2.4.3 Multiphoton imaging—Before imaging, the animal is anesthetized and a ring of low melting point wax (<52 °C) is applied around the coverslip to make a well for the dipping objective. The animal is placed either in a stereotaxic frame that fits into the microscope stage or screwed onto the head stabilizer on the stage using the metal bar implanted on the skull. The dipping objective is carefully lowered into a well of distilled water over the window being careful not to touch the objective to the wax ring or glass coverslip. Epi-fluorescence with a standard UV filter and a mercury lamp is used to focus on the surface of the brain. Care should be taken to limit the epi-fluorescence exposure to avoid photobleaching of the fluorescent dyes. Large blood vessels can be seen using epi-fluorescence as can labeled amyloid plaques, and an approximate imaging site can be chosen based on these markers.

For multiphoton imaging, the ideal laser excitation wavelength depends on the dyes used. For methoxy XO4 labeled plaques, thioflavin S labeled tangles, YFP, GFP, fluorescent indicator of caspase activation (FLICA), Texas red angiogram, and many other fluorophores, we find 800nm a suitable excitation wavelength. For each dye and combination of dyes, a scan of excitation wavelengths can be done to determine the best wavelength. We keep the laser power as low as possible while still detecting the signal to avoid photobleaching, particularly for repeat imaging experiments. Laser power is increased slightly as we image deeper into the cortex since photons are lost due to scattering of deep tissues. Photomultiplier tube gain and offset are adjusted to maximize clarity of signal at the beginning of experiments then the same settings are used throughout the experiment where possible. This is essential in studies such as those using the yellow cameleon calcium indicator which require precise calibration. Generally, a z-stack in 1–5 μm increments through the area of interest is obtained with an optical zoom of 3–5× using the 20× 0.95 NA

dipping objective to obtain a final resolution adequate for imaging pathology, cell bodies, and neurites.

2.4.4 Repeat imaging of the same sites—To re-image the same brain regions to track protein aggregation, neuronal degeneration, dendritic spine changes, etc., a low resolution image is taken with optical zoom 1 or 2× of each imaging site during the first imaging session. Using fiduciary markers such as the angiogram, large plaques, and the pattern of neurons or cell bodies, the same sites can be found again at 1 or 2× zoom. Stages with coordinate tracking systems can also be used to find the same sites, although since the animal might not be in exactly the same position in the stereotax at each imaging session, it is usually necessary to zero the coordinates on a large marker within each animal such as a large blood vessel draining into the superior saggital sinus.

2.5 Image analysis

To correct for breathing and heartbeat-induced motion artifacts, image stacks are aligned using the StackReg ImageJ plugin (Nathional Institutes of Health free software) (31). Other software can also be used to align and deconvolve images if necessary (for example autodeblur from AutoQuant). Images from multiple sessions can be aligned and compared to observe the formation of plaques and tangles and changes in surrounding neurons, dendritic spines, dystrophic neurites, neurite curvature, glia, reactive oxygen species, etc.

2.6 Troubleshooting

Several technical difficulties can arise with the surgical preparations and multiphoton imaging methods described here. During and shortly after cranial window implantation, excessive bleeding can occur resulting in morbidity or windows obscured by blood that preclude imaging. To minimize bleeding, careful drilling around the window without breaking the skull is important as is application of absorbent gel foam immediately after removing the skull flap. Even with clear imaging on the day of window implantation, some windows become occluded in the weeks after surgery due to thickening of the meninges. This can sometimes spontaneously recover allowing imaging in subsequent weeks. Inadequately securing the mouse's head in the stereotax results in large motion artifacts during imaging, thus we recommend tightening the ear bars if motion is detected when imaging small structures such as spines or using the system of securing the mouse by screwing to a metal bar implanted at the time of window implantation as described in section 2.3.3. A small amount of motion artifact can be compensated for using image stack alignment and deconvolution.

3. Discussion

We have used the methods described in this paper to investigate the formation of protein aggregates in AD models and many of their effects on structure and function of the brain as illustrated by the examples in figure 2. We have determined the time course of formation of senile plaques, NFT, and deposition of cerebral amyloid angiopathy, feats impossible without longitudinal in vivo imaging (9,24,32). We observed that both plaques and tangles can form within 24 hours, a remarkably fast time course that surprised many in the field since AD is such a slowly progressing disease.

Structural changes around plaques have been observed including formation of dystrophic neurites, neurite curvature, dendritic spine loss, decreased dendritic spine turnover, and accumulation of microglia around plaques (9,20,33). We have also observed degenerative changes associated with plaques such as increased reactive oxygen species (34), altered calcium dynamics (21,35), and calcineurin activation (22), which are thought to underlie the

structural changes in neurons surrounding plaques. Several treatments targeting amyloid plaques and their effects on neurons have been tried and the results observed over time in vivo including anti-Aβ antibodies to remove soluble and fibrillar Aβ (27,28,36), calcineurin inhibitors (22), and anti-oxidants (37,38); these treatments ameliorate to some degree the structural changes in neurites around plaques. These imaging experiments on APP mice have shown us that plaques form rapidly and precede the degeneration of neurites and synapses, and that these changes are reversible, lending support to the hypothesis that amyloid dysregulation and particularly soluble Aβ are early mediators of cognitive decline in AD that could be targeted therapeutically.

We have also begun to asses functional changes in the brain circuitry and how it is affected by plaques, including experiments with a CamKIIα-venus construct that is translocated to dendrites and translated in response to environmental stimulation (39). The function of neurons and astrocytes has also been observed using calcium imaging with yellow cameleon ratiometric dye introduced using AAV and Oregon Green Bapta dye introduced via micropipette injection (21,35). For in vivo imaging, ratiometric dyes to asses function are important since readouts that depend on intensity are very difficult to calibrate between animals. Each imaging site may be at slightly different cortical depth resulting in differing intensity of signal from the same absolute amount of fluorescence since light scattering means that deeper tissues are dimmer when imaged with the same laser intensity as more superficial sites. With ratiometric dyes, each image stack has its own internal control in the denominator of the ratio.

We also observed rapid formation of NFT which was surprisingly *preceded* by caspase activation (24). The rTg4510 model is known to undergo substantial neuronal loss as well as tangle formation (8,40), but cross-sectional studies cannot determine whether NFT-bearing neurons are the cells that die, or whether neurons without tangles are more likely to die. Using in vivo imaging, we have seen that caspases are activated and cellular membranes disrupted before NFT form but that NFT bearing neurons remain intact for many days, much longer than would be expected if they were dying of apoptosis (24,41). We continue to study the phenomena of tangle formation and neuronal death in this model using the uniquely appropriate method of observing neurons over time in the living brain.

In summary, there are many questions regarding protein aggregation and its toxicity in the AD brain which the method outlined here, in vivo multiphoton imaging, is ideally suited to address.

Acknowledgments

We gratefully acknowledge funding from the Alzheimer’s Association Zenith Award, NIH grants AG08487, K99AG33670, EB000768, and AG026249.

Abbreviations

AD	Alzheimer’s disease
Aβ	amyloid beta
NFT	neurofibrillary tangle
APP	amyloid precursor protein

References

1. Alzheimer A. Allgemeine Zeitschrift fur Psychiatrie und Psychisch-Gerichtliche Medizin 1907;64:146–48.
2. Gomez-Isla, T.; Spires, T.; de Calignon, A.; Hyman, BT. Handbook of clinical Neurology. Aminoff, MJ.; Boller, F.; Swaab, DF., editors. Vol. 89. Elsevier; Edinburgh: 2008.
3. Walsh DM, Selkoe DJ. J Neurochem 2007;101:1172–84. [PubMed: 17286590]
4. Gomez-Isla T, Hollister R, West H, Mui S, Growdon JH, Petersen RC, Parisi JE, Hyman BT. Ann Neurol 1997;41:17–24. [PubMed: 9005861]
5. Hsiao K, Chapman P, Nilsen S, Eckman C, Harigaya Y, Younkin S, Yang F, Cole G. Science 1996;274:99–102. [PubMed: 8810256]
6. Games D, Adams D, Alessandrini R, Barbour R, Berthelette P, Blackwell C, Carr T, Clemens J, Donaldson T, Gillespie F, et al. Nature 1995;373:523–7. [PubMed: 7845465]
7. Borchelt DR, Ratovitski T, van Lare J, Lee MK, Gonzales V, Jenkins NA, Copeland NG, Price DL, Sisodia SS. Neuron 1997;19:939–45. [PubMed: 9354339]
8. Santacruz K, Lewis J, Spires T, Paulson J, Kotilinek L, Ingelsson M, Guimaraes A, DeTure M, Ramsden M, McGowan E, Forster C, Yue M, Orne J, Janus C, Mariash A, Kuskowski M, Hyman B, Hutton M, Ashe KH. Science 2005;309:476–81. [PubMed: 16020737]
9. Meyer-Luehmann M, Spires-Jones TL, Prada C, Garcia-Alloza M, de Calignon A, Rozkalne A, Koenigsknecht-Talboo J, Holtzman DM, Bacskai BJ, Hyman BT. Nature 2008;451:720–4. [PubMed: 18256671]
10. Grinevich V, Kolleker A, Eliava M, Takada N, Takuma H, Fukazawa Y, Shigemoto R, Kuhl D, Waters J, Seeburg PH, Osten P. J Neurosci Methods 2009;184:25–36. [PubMed: 19628007]
11. Misgeld T, Kerschensteiner M, Bareyre FM, Burgess RW, Lichtman JW. Nat Methods 2007;4:559–61. [PubMed: 17558414]
12. Koenigsknecht-Talboo J, Meyer-Luehmann M, Parsadanian M, Garcia-Alloza M, Finn MB, Hyman BT, Bacskai BJ, Holtzman DM. J Neurosci 2008;28:14156–64. [PubMed: 19109498]
13. Holtmaat A, Bonhoeffer T, Chow DK, Chuckowree J, De Paola V, Hofer SB, Hubener M, Keck T, Knott G, Lee WC, Mostany R, Mrsic-Flogel TD, Nedivi E, Portera-Cailliau C, Svoboda K, Trachtenberg JT, Wilbrecht L. Nat Protoc 2009;4:1128–44. [PubMed: 19617885]
14. Hofer SB, Mrsic-Flogel TD, Bonhoeffer T, Hubener M. Nature 2009;457:313–17. [PubMed: 19005470]
15. Cabrales, P.; Carvalho, LJ. J Vis Exp. 2010.
16. Mostany, R.; Portera-Cailliau, C. J Vis Exp. 2008.
17. Golshani, P.; Portera-Cailliau, C. J Vis Exp. 2008.
18. Planel E, Richter KE, Nolan CE, Finley JE, Liu L, Wen Y, Krishnamurthy P, Herman M, Wang L, Schachter JB, Nelson RB, Lau LF, Duff KE. J Neurosci 2007;27:3090–7. [PubMed: 17376970]
19. Istaphanous GK, Loepke AW. Curr Opin Anaesthesiol 2009;22:368–73. [PubMed: 19434780]
20. Spires TL, Meyer-Luehmann M, Stern EA, McLean PJ, Skoch J, Nguyen PT, Bacskai BJ, Hyman BT. J Neurosci 2005;25:7278–87. [PubMed: 16079410]
21. Kuchibhotla KV, Goldman ST, Lattarulo CR, Wu HY, Hyman BT, Bacskai BJ. Neuron 2008;59:214–25. [PubMed: 18667150]
22. Wu HY, Hudry E, Hashimoto T, Kuchibhotla K, Rozkalne A, Fan Z, Spires-Jones T, Xie H, Arbel-Ornath M, Grosskreutz CL, Bacskai BJ, Hyman BT. J Neurosci 2010;30:2636–49. [PubMed: 20164348]
23. Tackenberg C, Brandt R. J Neurosci 2009;29:14439–50. [PubMed: 19923278]
24. de Calignon A, Fox LM, Pitstick R, Carlson GA, Bacskai BJ, Spires-Jones TL, Hyman BT. Nature 2010;464:1201–4. [PubMed: 20357768]
25. CDC, and NIH. U S Government Printing Office. 2007.
26. Spires-Jones TL, de Calignon A, Matsui T, Zehr C, Pitstick R, Wu HY, Osetek JD, Jones PB, Bacskai BJ, Feany MB, Carlson GA, Ashe KH, Lewis J, Hyman BT. J Neurosci 2008;28:862–7. [PubMed: 18216194]

27. Spires-Jones TL, Mielke ML, Rozkalne A, Meyer-Luehmann M, de Calignon A, Bacskai BJ, Schenk D, Hyman BT. Neurobiol Dis 2009;33:213–20. [PubMed: 19028582]
28. Bacskai BJ, Hickey GA, Skoch J, Kajdasz ST, Wang Y, Huang GF, Mathis CA, Klunk WE, Hyman BT. Proc Natl Acad Sci U S A 2003;100:12462–7. [PubMed: 14517353]
29. Velasco A, Fraser G, Delobel P, Ghetti B, Lavenir I, Goedert M. FEBS Lett 2008;582:901–6. [PubMed: 18291106]
30. Bacskai BJ, Kajdasz ST, McLellan ME, Games D, Seubert P, Schenk D, Hyman BT. J Neurosci 2002;22:7873–8. [PubMed: 12223540]
31. Thevenaz P, Ruttimann UE, Unser M. IEEE Trans Image Process 1998;7:27–41. [PubMed: 18267377]
32. Robbins EM, Betensky RA, Domnitz SB, Purcell SM, Garcia-Alloza M, Greenberg C, Rebeck GW, Hyman BT, Greenberg SM, Frosch MP, Bacskai BJ. J Neurosci 2006;26:365–71. [PubMed: 16407531]
33. Spires-Jones TL, Meyer-Luehmann M, Osetek JD, Jones PB, Stern EA, Bacskai BJ, Hyman BT. Am J Pathol 2007;171:1304–11. [PubMed: 17717139]
34. Garcia-Alloza M, Dodwell SA, Meyer-Luehmann M, Hyman BT, Bacskai BJ. J Neuropathol Exp Neurol 2006;65:1082–9. [PubMed: 17086105]
35. Kuchibhotla KV, Lattarulo CR, Hyman BT, Bacskai BJ. Science 2009;323:1211–5. [PubMed: 19251629]
36. Lombardo JA, Stern EA, McLellan ME, Kajdasz ST, Hickey GA, Bacskai BJ, Hyman BT. J Neurosci 2003;23:10879–83. [PubMed: 14645482]
37. Garcia-Alloza M, Borrelli LA, Rozkalne A, Hyman BT, Bacskai BJ. J Neurochem 2007;102:1095–104. [PubMed: 17472706]
38. Garcia-Alloza M, Prada C, Lattarulo C, Fine S, Borrelli LA, Betensky R, Greenberg SM, Frosch MP, Bacskai BJ. J Neurochem 2009;109:1636–47. [PubMed: 19457117]
39. Meyer-Luehmann M, Mielke M, Spires-Jones TL, Stoothoff W, Jones P, Bacskai BJ, Hyman BT. J Neurosci 2009;29:12636–40. [PubMed: 19812338]
40. Spires TL, Orne JD, SantaCruz K, Pitstick R, Carlson GA, Ashe KH, Hyman BT. Am J Pathol 2006;168:1598–607. [PubMed: 16651626]
41. de Calignon A, Spires-Jones TL, Pitstick R, Carlson GA, Hyman BT. J Neuropathol Exp Neurol 2009;68:757–61. [PubMed: 19535996]
42. Klunk WE, Bacskai BJ, Mathis CA, Kajdasz ST, McLellan ME, Frosch MP, Debnath ML, Holt DP, Wang Y, Hyman BT. J Neuropathol Exp Neurol 2002;61:797–805. [PubMed: 12230326]
43. Bacskai BJ, Klunk WE, Mathis CA, Hyman BT. J Cereb Blood Flow Metab 2002;22:1035–41. [PubMed: 12218409]
44. Christie RH, Bacskai BJ, Zipfel WR, Williams RM, Kajdasz ST, Webb WW, Hyman BT. J Neurosci 2001;21:858–64. [PubMed: 11157072]
45. Spires-Jones TL, Meyer-Luehmann M, Osetek JD, Jones PB, Stern EA, Bacskai BJ, Hyman BT. Am J Pathol 2007;171:1304–11. [PubMed: 17717139]
46. D'Amore JD, Kajdasz ST, McLellan ME, Bacskai BJ, Stern EA, Hyman BT. J Neuropathol Exp Neurol 2003;62:137–45. [PubMed: 12578223]
47. McLellan ME, Kajdasz ST, Hyman BT, Bacskai BJ. J Neurosci 2003;23:2212–7. [PubMed: 12657680]

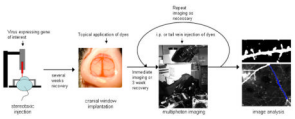

Figure 1.
Schematic of in vivo imaging.

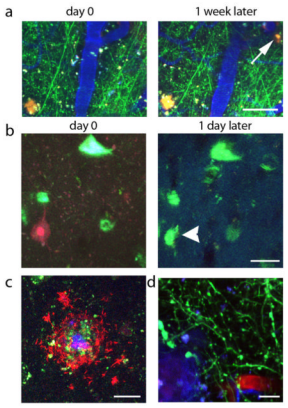

Figure 2.

Samples of data from in vivo imaging experiments in AD model mice. (a) shows an example of plaque formation (arrow points to new plaque, red) over 1 week with simultaneous imaging of YFP expressing neurites (green) and blood vessels (blue). We observe tangle formation (blue green, arrowhead points to new tangle labeled with thioflavin S in b) subsequent to caspase activation (red). We have also treated with anti Aβ antibodies (labeled with a red fluorophore, c), which decorate methoxy XO4 labeled dense cored plaques (blue/green). Dendritic spines loss has been observed in vivo (green, d) surrounding dense plaques (blue). Scale bars represent 50 μm (a), 20 μm (b, c), and 10 μm (d).

Table 1

Table of structures/processes imaged in vivo

Structure or process observed	Dye(s)/ transgenes	Reference(s)
Senile plaques	Thioflavin S, mehtoxy XO4, PIB	(28,42–44)
Neurofibrillary tangles	Thioflavin S, X34, FSB	(24,26,29)
microglia	Transgenic GFP microglia	(9,12)
Calcium concentration	Yellow chameleon, oregon green bapta	(21,35)
Mitochondria	Transgenic CFP mitochondria	(11)
Neurite structure (dendritic spines, dystrophies, curvature)	Transgenic YFP neurons, AAV injections of GFP, yellow chameleon	(9,20,34,36,45,46)
Neuronal nuclei	Hoescht	(24)
Cellular degeneration markers	PI, caspase indicators	(24,26,41)
Reactive oxygen species	H_2DCF, Amplex Red	(34,47)
Increased neuronal activity/ local translation in dendrites	CamKII-venus AAV	(39)